CHAPTER FOUR

Purification, reconstitution, and mass analysis of archaeal RNase P, a multisubunit ribonucleoprotein enzyme

Walter J. Zahurancik[a,b], Andrew S. Norris[a,b,c], Stella M. Lai[a,b,c], Dalton T. Snyder[a,c], Vicki H. Wysocki[a,b,c,*], and Venkat Gopalan[a,b,*]

[a]Department of Chemistry and Biochemistry, The Ohio State University, Columbus, OH, United States
[b]Center for RNA Biology, The Ohio State University, Columbus, OH, United States
[c]Resource for Native Mass Spectrometry-Guided Structural Biology, The Ohio State University, Columbus, OH, United States
*Corresponding authors: e-mail address: wysocki.11@osu.edu; gopalan.5@osu.edu

Contents

Abstract

The ubiquitous ribonucleoprotein (RNP) form of RNase P catalyzes the Mg^{2+}-dependent cleavage of the 5′ leader of precursor-transfer RNAs. The rate and fidelity of the single catalytic RNA subunit in the RNase P RNP is significantly enhanced by association with

Methods in Enzymology, Volume 659
ISSN 0076-6879
https://doi.org/10.1016/bs.mie.2021.07.006

protein cofactors. While the bacterial RNP exhibits robust activity at near-physiological Mg^{2+} concentrations with a single essential protein cofactor, archaeal and eukaryotic RNase P are dependent on up to 5 and 10 protein subunits, respectively. Archaeal RNase P—whose proteins share eukaryotic homologs—is an experimentally tractable model for dissecting in a large RNP the roles of multiple proteins that aid an RNA catalyst. We describe protocols to assemble RNase P from *Methanococcus maripaludis*, a methanogenic archaeon. We present strategies for tag-less purification of four of the five proteins (the tag from the fifth is removed post-purification), an approach that helps reconstitute the RNase P RNP with near-native constituents. We demonstrate the value of native mass spectrometry (MS) in establishing the accurate masses (including native oligomers and modifications) of all six subunits in *M. maripaludis* RNase P, and the merits of mass photometry (MP) as a complement to native MS for characterizing the oligomeric state of protein complexes. We showcase the value of native MS and MP in revealing time-dependent modifications (e.g., oxidation) and aggregation of protein subunits, thereby providing insights into the decreased function of RNase P assembled with aged preparations of recombinant subunits. Our protocols and cautionary findings are applicable to studies of other cellular RNPs.

1. Introduction

RNase P is an essential and ubiquitous ribonucleoprotein (RNP) complex that catalyzes Mg^{2+}-dependent cleavage of the 5′ leader of precursor-transfer RNAs (pre-tRNAs) (Altman, 2007; Esakova & Krasilnikov, 2010; Evans, Marquez, & Pace, 2006; Lai, Vioque, Kirsebom, & Gopalan, 2010). The RNase P RNP holoenzyme is comprised of a single catalytic RNase P RNA (RPR) that associates with a variable number of RNase P protein (RPP) subunits depending on the domain: 1 in bacteria, up to 5 in archaea, and up to 10 in eukarya (Esakova & Krasilnikov, 2010; Evans et al., 2006; Gopalan, Jarrous, & Krasilnikov, 2018; Lai et al., 2010). While the bacterial RPR in the absence of its single essential protein subunit is catalytically active, albeit at high ionic strength and Mg^{2+} concentrations, the cleavage activities of the archaeal and eukaryotic RPRs alone are considerably lower or, in some cases, undetectable (Guerrier-Takada, Gardiner, Marsh, Pace, & Altman, 1983; Kikovska, Svard, & Kirsebom, 2007; Pannucci, Haas, Hall, Harris, & Brown, 1999; Pulukkunat & Gopalan, 2008). However, in the presence of protein subunits, RNase P exhibits robust cleavage activity at lower Mg^{2+} concentrations (Guerrier-Takada et al., 1983; Lai et al., 2017; Pulukkunat & Gopalan, 2008; Sun & Harris, 2007; Tsai, Pulukkunat, Woznick, & Gopalan, 2006). With the multiprotein archaeal and eukaryotic RNase P, addition of one or more protein subunits

to the RNA results in fractional pre-tRNA cleavage activity compared to the complete holoenzyme, whereas the addition of all protein subunits restores full catalytic activity at near-physiological Mg^{2+} (Chen et al., 2012; Chen, Pulukkunat, Cho, Tsai, & Gopalan, 2010; Lai et al., 2017; Perederina, Berezin, & Krasilnikov, 2018). Thus, archaeal and eukaryotic RNase P are appealing models for investigating the individual and collective roles of multiple protein cofactors in aiding RNA catalysis.

To dissect the contributions of each of the RPPs to RNP holoenzyme assembly and to pre-tRNA substrate recognition and cleavage, it is essential to obtain homogeneous preparations of the RNA and protein subunits for subsequent reconstitution. Archaeal RNase P, which has fewer (albeit all homologous) protein subunits compared to the eukaryotic relative, is biochemically tractable *in vitro*. In fact, the RNase P holoenzymes from several archaea have been successfully reconstituted (Chen et al., 2010; Cho, Lai, Susanti, Mukhopadhyay, & Gopalan, 2010; Fukuhara et al., 2006; Kouzuma et al., 2003; Lai et al., 2017; Pulukkunat & Gopalan, 2008; Tsai et al., 2006). Pre-tRNA cleavage assays of step-wise assemblies of the RPR with partial and complete suites of all the recombinant protein subunits (POP5, RPP30, RPP21, RPP29, and L7Ae) helped establish the functional contributions of each RPP. Four of the five proteins operate as binary complexes: POP5·RPP30 and RPP21·RPP29 (Tsai et al., 2006). While POP5·RPP30 enhances the pre-tRNA cleavage rate, RPP21·RPP29 increases the binding affinity for substrate (Chen et al., 2010; Pulukkunat & Gopalan, 2008; Tsai et al., 2006). The fifth archaeal RPP, L7Ae, has been shown to further increase catalytic efficiency while reducing the Mg^{2+} ion requirement to near-cellular concentrations (Cho et al., 2010).

Here, we provide the protocols for *in vitro* reconstitution of RNase P from *Methanococcus maripaludis* (*M. maripaludis*), a methanogenic archaeon (Cho et al., 2010). We describe preparation of the RPR by T7 RNA polymerase (T7 RNAP)-catalyzed *in vitro* transcription (IVT) and present affinity tag-less strategies for purification of four of the five RPPs to minimize the potential interference of tags during reconstitution of the RNase P holoenzyme. We also describe a protocol for a pre-tRNA cleavage assay to measure the activity of the reconstituted enzyme. Although we detail assembly of a complete holoenzyme, partial assemblies (i.e., lacking some subunits) can be reconstituted similarly to determine the individual functional contributions of the proteins.

In addition, we highlight two methods for measuring the mass of macromolecules: native mass spectrometry (MS) and mass photometry (MP),

which offer a complementary, two-pronged approach to assess the quality of RNA/protein preparations and gain insights into the mechanism of time-dependent protein deactivation. The high mass accuracy of native MS enables detailed assessment of the quality of purified proteins by providing information on the accurate mass, oligomeric species present, and metal ion-binding states in a single experiment. Such details are not obtainable by sodium dodecyl sulfate-polyacrylamide gel electrophoresis (SDS-PAGE), the preferred method for validating protein purification despite its lower mass accuracy and inability to shed light on native assemblies or stoichiometries. Interestingly, reanalysis by native MS of aged RPP stocks (~1 year post-purification) revealed that the individual RPPs can become heavily modified (e.g., oxidation), which in turn may account for the observed activity loss upon long-term storage at −20 °C. An examination of the recently published cryo-electron microscopy structure of *Methanocaldococcus jannaschii* RNase P (Wan et al., 2019) provides hints as to possible protein folding or substrate-binding defects upon oxidation of select Cys, Met, and Trp residues in different RPPs.

On the other hand, MP, whose measurements are of lower mass accuracy than native MS, can be used to readily gain information on the oligomeric state of proteins either alone or in complexes (Soltermann et al., 2020; Sonn-Segev et al., 2020). Unlike native MS, MP is compatible with non-volatile salts, such as those that are typically included in storage or assay buffers (e.g., Mg^{2+} and Tris). Thus, MP can be used to assess the oligomeric distribution of proteins under buffer conditions and, notably, at RPP concentrations identical to those used in activity assays. We find that the oligomeric states detected in two different preparations of POP5·RPP30 correlate with their activity differences. SDS-PAGE was predictably unable to discern the full range of nonnative oligomeric states in these protein preparations, although faint bands corresponding to putative heterodimers could be observed even under denaturing conditions (see Sections 3.6 and 5).

Overall, although we have provided protocols for assembly and functional testing of *M. maripaludis* RNase P, our approaches can be easily adapted and the insights applied to other cellular RNPs.

2. Materials

All protein overexpression (Section 2.2), purification (Section 2.3), native MS (Section 2.4), and mass photometry (Section 2.6) solutions should be prepared using reverse osmosis-filtered or double distilled/deionized

water (ddH_2O). *In vitro* transcription (Section 2.1) and cleavage assay (Section 2.5) solutions should be prepared using autoclaved ddH_2O.

2.1 *In vitro* transcription (IVT) of *Methanococcus maripaludis* RNase P RNA (RPR)

1. 10× T7 RNA polymerase (RNAP) IVT buffer: 400 mM Tris-HCl, pH 7.6 at room temperature (RT; typically 20–23 °C); 240 mM $MgCl_2$; 20 mM spermidine; 0.1% (v/v) Triton X-100
2. 100 mM dithiothreitol (DTT), dissolved in ddH_2O and stored at −20 °C (see Note 1)
3. Nucleoside triphosphate (NTP) mix (25 mM each), diluted in ddH_2O (see Notes 2 and 3)
4. T7 RNAP IVT template (see Note 4). The template used to transcribe *M. maripaludis* RPR was prepared as described previously (Cho et al., 2010)
5. Thermostable inorganic pyrophosphatase (TIPP; New England Biolabs), diluted to 0.2 U/μL in 1× T7 RNAP IVT buffer and 10% (v/v) glycerol
6. T7 RNAP (see Note 5)
7. 1× Tris-boric acid-ethylenediaminetetraacetic acid (TBE; 89 mM Tris base, 89 mM boric acid, 2 mM EDTA)
8. 2% (w/v) agarose gel (0.6 g agarose per 30 mL 1× TBE)
9. DNase I (10 U/μL; Roche)
10. Buffer-saturated phenol, pH 7.9 (IBI Scientific)
11. Chloroform, ≥99.9% (MilliporeSigma)
12. 3500 Da molecular weight cut-off (MWCO) dialysis tubing (BioDesign Inc., New York)
13. 3 M sodium acetate, pH 5.2
14. 100% (v/v) ethanol
15. 75% (v/v) ethanol

2.2 Overexpression of *M. maripaludis* RNase P proteins (RPPs)

1. Appropriate overexpression strains: in this protocol, the following strains of *Escherichia coli* were used:
   a. BL21(DE3) (Studier & Moffatt, 1986)
   b. BL21(DE3) Rosetta (Novagen)
2. Recombinant plasmids containing genes encoding *M. maripaludis* RPPs under the control of a T7 promoter (see Note 6) (Lai et al., 2021): the

recombinant plasmids used in this protocol were described previously (Cho et al., 2010):

a. pLANT-2b–POP5·RPP30
b. pLANT-2b–RPP21
c. pET-15b–$(His)_6$-RPP29 (a thrombin cleavage site is included to allow removal of the $(His)_6$ tag)
d. pET-15b–L7Ae

3. Miller's LB: Add 2.5 g tryptone, 2.5 g NaCl, 1.25 g yeast extract per 250 mL ddH_2O. Sterilize by autoclaving
4. LB agar: Add 1.5 g agar per 100 mL Miller's LB. Sterilize by autoclaving
5. Antibiotics, prepared as described and stored at −20 °C
   a. 35 mg/mL chloramphenicol, dissolved in 100% methanol
   b. 35 mg/mL kanamycin, dissolved in ddH_2O
   c. 100 mg/mL carbenicillin, dissolved in 100% methanol
6. 40% (w/v) glucose, dissolved in ddH_2O and filter sterilized
7. 1 M isopropyl β-D-1-thiogalactopyranoside (IPTG; GoldBio), dissolved in ddH_2O and stored at −20 °C
8. 100 mM $ZnCl_2$

2.3 Purification of *M. maripaludis* RPPs

2.3.1 Purification of POP5·RPP30

1. POP5·RPP30/RPP21 lysis buffer: 25 mM Tris-HCl, pH 8 at RT; 5 mM DTT; 1 mM EDTA; 0.1 mM phenylmethylsulfonyl fluoride (PMSF); 1 M NaCl
2. Sonicator [e.g., Q125 Sonicator (Qsonica)]
3. 10% (v/v) polyethyleneimine (PEI), diluted in ddH_2O and pH adjusted to 8 (see Note 7)
4. Finely crushed $(NH_4)_2SO_4$
5. Ion-exchange (IEX) buffer A: 25 mM Tris-HCl, pH 8 at RT; 5 mM DTT; 1 mM EDTA; 0.1 mM PMSF
6. 0.4 μm syringe filters (VWR International)
7. 1 mL HiTrap SP (Sulfopropyl)-Sepharose FF column (Cytiva; see Note 8)
8. IEX buffer B: 25 mM Tris-HCl, pH 8 at RT; 5 mM DTT; 1 mM EDTA; 0.1 mM PMSF; 2 M NaCl
9. 15% (w/v) polyacrylamide (37.5:1 acrylamide:bisacrylamide), 0.4% (w/v) sodium dodecyl sulfate (SDS) gel
10. 1 mL HiTrap Phenyl HP column (Cytiva; see Note 8)

11. 3000 Da MWCO centrifugal concentrators [e.g., Amicon Ultra-15 (MilliporeSigma)]
12. 3500 Da MWCO dialysis tubing (BioDesign Inc., New York)
13. RPP storage buffer: 50 mM HEPES-KOH, pH 8 at RT; 500 mM ammonium acetate; 7.5 mM $MgCl_2$
14. 100% (v/v) glycerol

2.3.2 Purification of RPP21

1. 1 mL HiTrap Heparin HP column (Cytiva; see Note 8)
2. See Section 2.3.1 for a list of other common purification materials

2.3.3 Purification of RPP29

1. RPP29 buffer A: 25 mM Tris-HCl, pH 8 at RT; 1 mM EDTA; 500 mM NaCl; 10 mM imidazole
2. 1 mL HisTrap HP column (Cytiva; see Note 8)
3. RPP29 buffer B: 25 mM Tris-HCl, pH 8 at RT; 1 mM EDTA; 500 mM NaCl; 1 M imidazole
4. 1× phosphate buffered saline (PBS): 137 mM NaCl; 2.7 mM KCl; 10 mM Na_2HPO_4; 1.7 mM KH_2PO_4; pH 7.4
5. Thrombin (1 U/μL; Cytiva)
6. See Section 2.3.1 for a list of other common purification materials

2.3.4 Purification of L7Ae

1. L7Ae lysis buffer: 100 mM Tris-HCl, pH 9 at RT; 5 mM DTT; 0.1 mM PMSF
2. L7Ae IEX buffer A: 25 mM Tris-HCl, pH 8 at RT; 1 mM DTT; 1 mM EDTA; 0.1 mM PMSF
3. 1 mL HiTrap Q (quaternary ammonium) FF column (Cytiva; see Note 8)
4. L7Ae IEX buffer B: 25 mM Tris-HCl, pH 8 at RT; 1 mM DTT; 1 mM EDTA; 0.1 mM PMSF; 2 M NaCl
5. 18% (w/v) polyacrylamide (37.5:1 acrylamide:bisacrylamide), 0.4% (w/v) SDS gel
6. See Section 2.3.1 for a list of other common purification materials

2.4 Validation of RPR and RPPs by native MS

1. Pierce 96-well microdialysis plate, 3500 Da MWCO (Thermo Fisher Scientific)
   Alternative: Micro Bio-Spin P6 column (Bio-Rad Laboratories)

2. 500 mM ammonium acetate, 99.99% (MilliporeSigma)
3. 0.4 mM magnesium acetate
4. 0.5–10 μL μltra Micro Gel Tip (Genesee Scientific)
   Alternative: Hamilton Syringe (10 μL, cemented needle, 26 gauge, 2 in. needle)
5. Borosilicate filament capillaries, OD 1.0 mm, ID 0.78 mm (Sutter Instrument)
6. P-97 Flaming/Brown Micropipette Puller (Sutter Instrument)
7. Nanospray Flex ion source fitted with a platinum wire electrode (Thermo Fisher Scientific)
8. Exactive Extended Mass Range (EMR) mass spectrometer (Thermo Fisher Scientific) modified with quadrupole
   Alternative: Q Exactive Ultra-High Mass Range (UHMR) mass spectrometer (Thermo Fisher Scientific) or other mass spectrometers, with their compatible sources optimized for native MS.

2.5 Reconstitution of *M. maripaludis* RNase P

1. 2× assay buffer: 100 mM Tris-HCl, pH 7.5 at 37 °C; 1 M NH_4OAc; 15 mM $MgCl_2$
2. RPP dilution buffer: 50 mM Tris-HCl, pH 7.5 at 37 °C; 500 mM NH_4OAc; 7.5 mM $MgCl_2$; 5% (v/v) glycerol
3. 50% (v/v) glycerol
4. 2 mg/mL bovine serum albumin (BSA; Pierce)
5. Pre-tRNA substrate (see Note 9), both unlabeled and radiolabeled (see Notes 10 and 11)
6. Quench dye: 7 M urea, 10% (v/v) phenol, 0.04% (w/v) bromophenol blue, 0.04% (w/v) xylene cyanol
7. 8% (w/v) polyacrylamide (19:1 acrylamide:bisacrylamide), 7 M urea gel
8. Storage phosphor screen (Cytiva)
9. Laser scanner with phosphor imaging mode [e.g., Typhoon RGB (Cytiva)]

2.6 Assessing RPP oligomerization by mass photometry

1. Refeyn One™ mass photometry system (Refeyn)
2. Precision cover glasses, #1.5H Thickness, 24 × 50 mm (Thorlabs)
3. Water bath sonicator
4. 50% (v/v) methanol
5. 100% (v/v) methanol

6. Nitrogen gas, industrial grade
7. CultureWell™ reusable gaskets, 50-3 mm diameter, 1 mm depth (3–10 μL) (Grace Bio-Labs)
8. 100% (v/v) isopropyl alcohol
9. IMMOIL-F30CC low autofluorescence immersion oil (Olympus)

3. Methods

3.1 *In vitro* transcription (IVT) of *Methanococcus maripaludis* RNase P RNA (RPR)

1. Prepare the IVT reaction mix. An example IVT reaction mix is tabulated below:

Component	Initial concentration	Volume (μL)	Final concentration
T7 RNAP IVT buffer	10×	10	1×
DTT	100 mM	10	10 mM
NTP mix	25 mM each	20	5 mM each
TIPP	0.2 U/μL	0.5	0.001 U/μL
T7 RNAP IVT template	See Note 12		
T7 RNAP	See Note 5		
ddH_2O	Adjust reaction to final volume of 100 μL		

2. Incubate the reaction for 3–4 h at 37 °C.
3. Check for successful transcription of the RPR by electrophoresing 1 μL of the IVT reaction on a 2% (w/v) agarose gel (see Note 13), using 1× TBE as running buffer.
4. After verifying synthesis of the expected RPR product, add DNase I (10 U per 100 μL IVT reaction) to the transcription reaction and incubate for 1 h at 37 °C.
5. Add 1/2 volume each of phenol and chloroform to the transcription reaction, vortex vigorously, and centrifuge for 5 min at 20,000 × *g*.
6. Remove the top aqueous phase, and transfer it to a clean tube.
7. Add 1 volume of chloroform to the isolated aqueous phase, vortex vigorously, and centrifuge for 5 min at 20,000 × *g*.
8. Remove the top aqueous phase, and transfer it to a clean tube.

9. Adjust the volume of the isolated aqueous phase to 300 μL with ddH_2O.
10. Transfer the sample to dialysis tubing (3500 Da MWCO), and dialyze extensively against ddH_2O (at least 3×4 L; the final round of dialysis should continue for at least 16 h).
11. Recover the sample from dialysis, and transfer it to a clean tube.
12. Add 1/10 volume 3 M sodium acetate (pH 5.2) and 2.5 volumes 100% (v/v) EtOH and mix well. Optional: If the RNA yield is expected to be low, add 1/100 volume 20 mg/mL glycogen and/or incubate the mixture at −80 °C for at least 1 h to improve visualization of the RNA pellet.
13. Thaw the sample, and centrifuge for 5 min at $20{,}000 \times g$.
14. Carefully withdraw the solution without disturbing the pellet. Wash the pellet with 70% (v/v) EtOH. Vortex vigorously, and centrifuge for 5 min at $20{,}000 \times g$. Then carefully withdraw the solution. Perform at least two EtOH washes in this manner (see Note 14).
15. Allow the pellet to dry, and then resuspend it in ddH_2O. Vortex vigorously to ensure complete resuspension.
16. Calculate the concentration of the resuspended RPR by measuring A_{260} (calculated $\varepsilon = 2{,}561{,}700\ M^{-1}\ cm^{-1}$).
17. Store at −20 °C.

3.2 Overexpression of *M. maripaludis* RNase P proteins (RPPs)

1. Transform the appropriate strain of *E. coli* competent cells with a single plasmid containing a gene encoding one (two in the case of POP5·RPP30) of the *M. maripaludis* RPPs.
   a. BL21(DE3) cells are used for overexpression of POP5·RPP30 and RPP21.
   b. BL21(DE3) Rosetta cells are used for overexpression of RPP29 and L7Ae.
2. Plate the transformation reaction on LB agar plates supplemented with either 35 μg/mL kanamycin (POP5·RPP30 and RPP21) or 35 μg/mL chloramphenicol and 100 μg/mL carbenicillin (RPP29 and L7Ae). Incubate the plate overnight at 37 °C.
3. Start a seed culture by inoculating 2 mL LB media [supplemented with appropriate antibiotics and 1% (w/v) glucose (see Note 15)] with a single transformant.
4. Shake the seed culture for 15–16 h at 37 °C.

5. Start a large overexpression culture by inoculating 250 mL LB media (supplemented with appropriate antibiotics) with 2.5 mL of seed culture.
6. Shake the overexpression culture at 37 °C until the OD_{600} reaches ~0.5 (about 2–2.5 h).
7. Induce overexpression with the addition of the appropriate amount of IPTG inducer.
   a. Overexpression of POP5·RPP30 or L7Ae is initiated by addition of 2 mM IPTG.
   b. Overexpression of RPP21 or RPP29 is initiated by addition of 0.5 mM IPTG. For RPP21, 1 mM $ZnCl_2$ (final concentration) is also added to the overexpression culture at the time of IPTG addition.
8. Continue shaking the overexpression culture under previously optimized conditions.
   a. Cultures for POP5·RPP30 and L7Ae are shaken for 4 h at 37 °C.
   b. Cultures for RPP21 and RPP29 are shaken for 15 h at 21 °C.
9. Following overexpression, harvest the cells by centrifugation for 10 min at 5000 × *g*.
10. Divide the resulting pellet into 2 × 125-mL pellets, and freeze them at −80 °C until ready to use.

3.3 Purification of *M. maripaludis* RPPs

3.3.1 Purification of POP5·RPP30

1. Remove a single 125-mL pellet from −80 °C, and thaw on ice.
2. Once thawed, resuspend the pellet in 25 mL POP5·RPP30/RPP21 lysis buffer.
3. Lyse the resuspended cells by sonicating for a total on-time of 6 min at 50% amplitude with pulse cycles of 5 s on and 2 s off. Keep the cells on ice during sonication.
4. Centrifuge the lysate for 15 min at 12,000 × *g* and 4 °C.
5. Transfer the cleared lysate to a clean 50 mL Erlenmeyer flask, and incubate for 15 min at 65 °C.
6. Centrifuge the sample for 15 min at 12,000 × *g* and 4 °C.
7. Transfer the supernatant to a clean tube, and add 0.05% (v/v) PEI (final concentration). Incubate on ice for 20 min (see Note 7).
8. Centrifuge the suspension for 15 min at 12,000 × *g* and 4 °C.
9. Transfer the supernatant to a clean beaker, and place on ice.

10. Slowly add finely crushed $(NH_4)_2SO_4$ with stirring until the solution reaches 80% saturation. After the addition of $(NH_4)_2SO_4$, continue stirring on ice for an additional 15 min.
11. Centrifuge the suspension for 15 min at $12{,}000 \times g$ and 4 °C (see Note 16).
12. Remove the supernatant and resuspend the pellet in 20 mL IEX buffer A.
13. Filter the solution using a 0.4 μm syringe filter to remove any undissolved particulate.
14. Load the sample onto a 1 mL HiTrap SP FF column using a syringe or a peristaltic pump, and collect the flowthrough.
15. Wash the column with 10 column volumes (CVs) IEX buffer A, and collect the flowthrough.
16. Attach the column to an FPLC, and wash it as follows:
    a. 5 CV IEX buffer A
    b. 5 CV gradient to 25% IEX buffer B
    c. 20 CV gradient to 60% IEX buffer B
17. Use the UV absorbance profile to identify the peak fractions, and test aliquots from these fractions on a 15% (w/v) polyacrylamide (37.5:1 acrylamide:bisacrylamide), 0.4% (w/v) SDS gel.
18. Pool the fractions with the highest concentration of POP5·RPP30 and the fewest impurities. POP5·RPP30 typically elutes between 600 and 750 mM NaCl.
19. Adjust the NaCl concentration to 2 M by adding solid NaCl and nutating gently until all the solid NaCl dissolves.
20. Load the sample onto a 1 mL HiTrap Phenyl HP column using a syringe or a peristaltic pump, and collect the flowthrough.
21. Wash the column with 10 CVs of IEX buffer B, and collect the flowthrough.
22. Attach the column to an FPLC, and wash it with a 20 CV gradient to 0% IEX buffer B.
23. Use the UV absorbance profile to identify the peak fractions, and test aliquots from these fractions on a 15% (w/v) polyacrylamide (37.5:1 acrylamide:bisacrylamide), 0.4% (w/v) SDS gel.
24. Pool the peak fractions as above. POP5·RPP30 typically elutes as a single peak between 1300 and 600 mM NaCl.
25. Concentrate the protein as desired using a centrifugal concentrator (see Note 17).
26. Transfer the protein to dialysis tubing (3500 Da MWCO), and dialyze against RPP storage buffer (500 mL) at 4 °C for 2 h. Replace the buffer, and allow the second round of dialysis to continue overnight.

27. Recover the sample, and calculate the protein concentration by measuring A_{280} (calculated ε for POP5·RPP30 = 41,830 M^{-1} cm^{-1}).
28. Add glycerol to a final concentration of 25% (v/v).
29. Aliquot and store at −20 °C.

3.3.2 Purification of RPP21

1. Remove a single 125-mL pellet from −80 °C and thaw on ice.
2. Once thawed, resuspend the pellet in 25 mL POP5·RPP30/RPP21 lysis buffer.
3. Lyse the resuspended cells by sonicating for a total on-time of 6 min at 50% amplitude with pulse cycles of 5 s on and 2 s off. Keep the cells on ice during sonication.
4. Centrifuge the lysate for 15 min at 12,000 × *g* and 4 °C.
5. Transfer the sample to a clean tube, and add 0.05% (v/v) PEI (final concentration). Incubate on ice for 20 min (see Note 7).
6. Centrifuge the suspension for 15 min at 12,000 × *g* and 4 °C.
7. Transfer the supernatant to a clean beaker, and place on ice.
8. Slowly add finely crushed $(NH_4)_2SO_4$ with stirring until the solution reaches 60% saturation. After the addition of $(NH_4)_2SO_4$, continue stirring on ice for an additional 15 min.
9. Centrifuge the suspension for 15 min at 12,000 × *g* and 4 °C (see Note 16).
10. Remove the supernatant, and resuspend the pellet in 20 mL IEX buffer A.
11. Filter the solution using a 0.4-μm syringe filter to remove any undissolved particulate.
12. Load the sample onto a 1 mL HiTrap Heparin HP column using a syringe or a peristaltic pump, and collect the flowthrough.
13. Wash the column with 10 CV of IEX buffer A and collect the flowthrough.
14. Attach the column to an FPLC and wash it as follows:
    a. 20 CV gradient to 50% IEX buffer B
    b. 10 CV gradient to 100% IEX buffer B
15. Use the UV absorbance profile to identify the peak fractions, and test aliquots from these fractions on a 15% (w/v) polyacrylamide (37.5:1 acrylamide:bisacrylamide), 0.4% (w/v) SDS gel.
16. Pool the fractions with the highest concentration of RPP21 and the fewest impurities. RPP21 typically elutes between 750 and 1000 mM NaCl.

17. Adjust the NaCl concentration to 2 M by adding solid NaCl and nutating gently until all the solid NaCl dissolves.
18. Load the sample onto a 1 mL HiTrap Phenyl HP column using a syringe or a peristaltic pump, and collect the flowthrough.
19. Wash the column with 10 CV of IEX buffer B, and collect the flowthrough.
20. Attach the column to an FPLC and wash it as follows:
    a. 5 CV gradient to 50% IEX buffer B
    b. 10 CV gradient to 0% IEX buffer B
21. Identify and test peak fractions as in Step 15.
22. Pool the fractions with the highest concentration of RPP21 and the fewest impurities. RPP21 typically elutes at <500 mM NaCl.
23. Concentrate the protein as desired using a centrifugal concentrator (see Note 17).
24. Transfer the protein to dialysis tubing (3500 Da MWCO), and dialyze against RPP storage buffer (500 mL) at 4 °C for 2 h. Replace the buffer, and allow the second round of dialysis to continue overnight.
25. Recover the sample and calculate the protein concentration by measuring A_{280} (calculated $\varepsilon = 11{,}460\,M^{-1}\,cm^{-1}$).
26. Add glycerol to a final concentration of 25% (*v*/v).
27. Aliquot and store at −20 °C.

3.3.3 Purification of RPP29

1. Remove a single 125-mL pellet from −80 °C and thaw on ice.
2. Once thawed, resuspend the pellet in 25 mL RPP29 buffer A.
3. Lyse the resuspended cells by sonicating for a total on-time of 6 min at 50% amplitude with pulse cycles of 5 s on and 2 s off. Keep the cells on ice during sonication.
4. Centrifuge the lysate for 15 min at 12,000 × *g* and 4 °C.
5. Transfer the sample to a clean tube, and add 0.05% (v/v) PEI (final concentration). Incubate on ice for 20 min (see Note 7).
6. Centrifuge the suspension for 15 min at 12,000 × *g* and 4 °C.
7. Transfer the supernatant to a clean tube, and filter it using a 0.4 μm syringe filter to remove any particulate.
8. Load the sample onto a 1 mL HisTrap HP column using a syringe or a peristaltic pump, and collect the flowthrough.
9. Attach the column to an FPLC and wash it as follows:
    a. 5 CV RPP29 buffer A
    b. 10 CV gradient to 50% RPP29 buffer B

c. 6 CV 50% RPP29 buffer B

10. Use the UV absorbance profile to identify the peak fractions, and test aliquots from these fractions on a 15% (w/v) polyacrylamide (37.5:1 acrylamide:bisacrylamide), 0.4% (w/v) SDS gel.
11. Pool the fractions with the highest concentration of RPP29 and the fewest impurities. RPP29 typically elutes at >200 mM imidazole. Estimate protein concentration by measuring A_{280} (calculated $\varepsilon = 2980\ M^{-1}\ cm^{-1}$; see Note 18).
12. Transfer the protein to dialysis tubing (3500 Da MWCO), and dialyze against 500 mL 1× PBS for 1.5 h at RT (see Note 19).
13. Open the dialysis bag, and add thrombin (at least one unit per 100 μg protein; see manufacturer's instructions).
14. Resume dialysis against 500 mL fresh 1× PBS for 2.5 h at RT, and then continue dialyzing overnight at 4 °C.
15. Check for the extent of cleavage by thrombin on a 15% (w/v) polyacrylamide (37.5:1 acrylamide:bisacrylamide), 0.4% (w/v) SDS gel.
16. Concentrate the protein as desired using a centrifugal concentrator (see Note 17).
17. Transfer the protein to dialysis tubing (3500 Da MWCO), and dialyze against RPP storage buffer (500 mL) at 4 °C for 2 h. Replace the buffer, and allow the second round of dialysis to continue overnight.
18. Recover the sample and calculate the protein concentration by measuring A_{280} (calculated $\varepsilon = 2980\ M^{-1}\ cm^{-1}$; see Note 18).
19. Add glycerol to a final concentration of 25% (v/v).
20. Aliquot and store at −20 °C.

3.3.4 Purification of L7Ae

1. Remove a single 125-mL pellet from −80 °C and thaw on ice.
2. Once thawed, resuspend the pellet in 25 mL L7Ae lysis buffer.
3. Lyse the resuspended cells by sonicating for a total on-time of 6 min at 50% amplitude with pulse cycles of 5 s on and 2 s off. Keep the cells on ice during sonication.
4. Centrifuge the lysate for 15 min at 12,000 × *g* and 4 °C.
5. Transfer the cleared lysate to a clean 50 mL Erlenmeyer flask, and incubate for 15 min at 65 °C.
6. Centrifuge the sample for 15 min at 12,000 × *g* and 4 °C.
7. Transfer the supernatant to a clean tube, and add 0.05% (v/v) PEI (final concentration). Incubate on ice for 20 min (see Note 7).
8. Centrifuge the suspension for 15 min at 12,000 × *g* and 4 °C.

9. Transfer the supernatant to a clean tube, and filter it using a 0.4 μm syringe filter to remove any particulate.
10. Load the sample onto a 1 mL HiTrap Q FF column using a syringe or a peristaltic pump, and collect the flowthrough.
11. Wash the column with 10 CV of L7Ae IEX buffer A, and collect the flowthrough.
12. Attach the column to an FPLC and wash it with a 20 CV gradient to 25% L7Ae IEX buffer B.
13. Check the UV peak fractions on an 18% (w/v) polyacrylamide (37.5:1 acrylamide:bisacrylamide), 0.4% (w/v) SDS gel.
14. Pool the fractions with the highest concentration of L7Ae and the fewest impurities. L7Ae typically elutes at 200–360 mM NaCl.
15. Adjust the NaCl concentration to 2 M by adding solid NaCl and nutating gently until all the solid NaCl dissolves.
16. Load the sample onto a 1 mL HiTrap Phenyl HP column using a syringe or a peristaltic pump, and collect the flowthrough.
17. Wash the column with 10 CV of IEX buffer B, and collect the flowthrough.
18. Verify the presence of L7Ae in the load and wash flowthrough by checking the fractions as in Step 13.
19. Pool the load and wash flowthrough fractions, and concentrate the protein as desired using a centrifugal concentrator (see Note 17).
20. Transfer the protein to dialysis tubing (3500 MWCO) and dialyze against RPP storage buffer (500 mL) at 4 °C for 2 h. Replace the buffer, and allow the second round of dialysis to continue overnight.
21. Recover the sample and calculate the protein concentration by measuring A_{280} (calculated $\varepsilon = 4470\,M^{-1}\,cm^{-1}$; see Note 19).
22. Add glycerol to a final concentration of 25% (v/v).
23. Aliquot and store at −20 °C.

3.4 Validation of RPR and RPPs by native MS

1. Remove the RPR and RPP stocks from −20 °C, and thaw. The RPR can be thawed at RT, while the RPPs should remain on ice.
2. Dilute the RPR to 1 μM using 500 mM ammonium acetate, 0.4 mM magnesium acetate.
3. Transfer an aliquot of each RPP stock into individual microdialysis devices (3500 Da MWCO), and dialyze them against 500 mM ammonium acetate in a 96-deep-well plate or in a 2-mL centrifuge tube.

Change the well solution once every hour for up to 8 changes. If needed, dialysis can continue overnight (see Note 20).

4. Recover the dialyzed protein solutions and measure their concentrations (see Sections 3.3.1–3.3.4).
5. Dilute each of the RPPs to 1–10 μM using native MS solution.
6. Pull multiple glass emitters with the micropipette puller (Fig. 1). Emitter pulling parameters for a P-97 Flaming/Brown Micropipette Puller can vary (see user manual). An example of parameter ranges is given below:

Parameter	Setting
Heat	[a]Ramp heat ± 10
Pull	15–25
Velocity	15–25
Delay (ms)	150–250

[a]Determined by conducting a pilot ramp test.

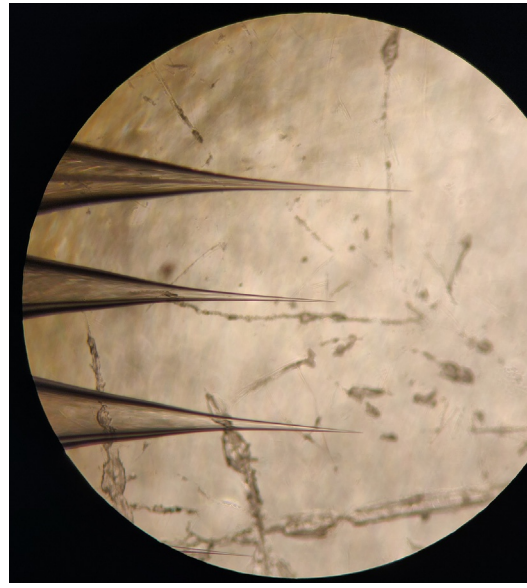

Fig. 1 Fourfold magnification of the tips of emitters. Nano electrospray emitters with a tip shape as shown generally work well at the spray voltages specified in Table 1.

7. Pipette (Ultra Micro Gel Tip) 2–5 μL of an RPR or RPP dilution into a glass emitter (see Note 21).
8. Load the emitter onto the platinum wire that is fitted to the Nanospray Flex ion source.
9. Place the tip of the emitter centered and less than 1 cm from the front of the inlet of the mass spectrometer.
10. Adjust the spray voltage between 0.6 and 1.3 kV until stable signal is observed. The EMR mass spectrometer tune settings for positive ion mode electrospray ionization are detailed in Table 1.
11. Record the full mass spectrum for each sample in this fashion (Fig. 2). Collisional activation may be used as needed (see Note 22).
12. For protein complexes such as POP5·RPP30, adjust higher-energy collisional dissociation (HCD) voltage to cause complexes to dissociate into constituent proteins so that their masses may be measured accurately (see Note 22). Record the resulting dissociation spectrum (Fig. 2E).

Table 1 EMR mass spectrometer tune settings used in this method.

Setting	Value	Notes
Spray voltage (kV)	0.7–0.8	First increase spray voltage past the recommended range, then gradually decrease it until a stable signal is observed
Capillary temperature (°C)	250	
S-Lens RF level (V)	200	
Injection flatapole DC (V)	12	
Bent flatapole DC (V)	10	
Inter flatapole lens (V)	8	
HCD direct eV (V)	1	Higher HCD voltages can be used for fragmentation and for de-adducting
Inject time (ms)	200	
Microscans	2	
Scan range (m/z)	1000–10,000	
Resolution (at 200 m/z)	8750	Adjust to higher resolution to resolve isotopic peaks
Trapping gas pressure	4–6	Use larger values to improve higher m/z transmission

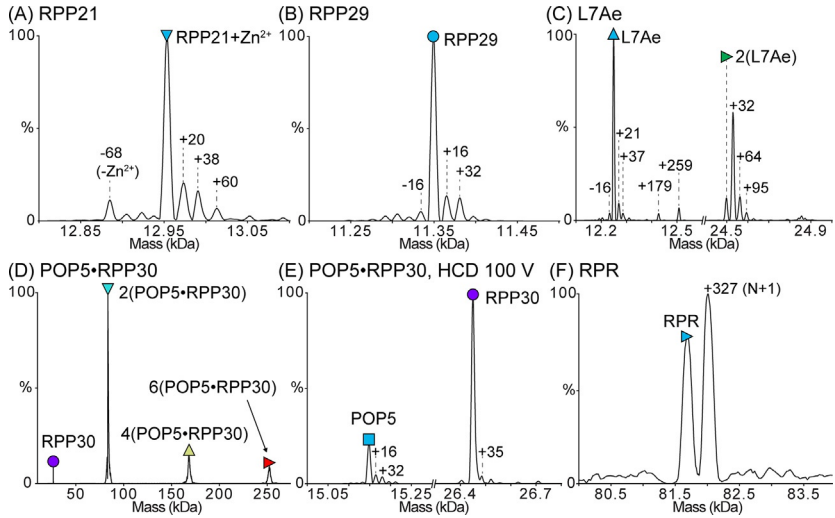

Fig. 2 Deconvolved zero-charge mass spectra of the purified *M. maripaludis* RNase P subunits. Proteins were dialyzed into 500 mM ammonium acetate prior to analysis. In each spectrum, the peak corresponding to the mass of the full-length subunit is indicated with a symbol. The expected and observed masses of each subunit are reported in Table 3. (A) Mass spectrum of RPP21 bound to Zn^{2+}. Only a small population of RPP21 is Zn^{2+}-free, indicating that Zn^{2+} remains tightly bound to RPP21 during all purification steps. (B) Mass spectrum of RPP29. (C) Mass spectrum of L7Ae. L7Ae readily forms a disulfide-mediated homodimer, which is lost upon treatment with DTT. The single-Cys-mediated dimer is also supported by the inability to dissociate it using HCD. (D) Mass spectrum of POP5·RPP30. This binary complex forms the expected heterotetramer [$(POP5{\cdot}RPP30)_2$] in addition to some higher-order oligomers. (E) Dissociation of the heterotetramer in (D) yields species with the expected masses for POP5 and RPP30. (F) Mass spectrum of RPR in 500 mM ammonium acetate and 0.4 mM magnesium acetate. Both the target RNA species (N) and a species extended by a single nucleotide (N + 1), which is typical of T7 RNAP IVT, are observed. The mass spectrum confirms that the RPR is a mix of N and N + 1 species with few contaminants (if any), suggesting that the doublet observed in a 2% (w/v) agarose gel likely results from alternative RPR conformations (see Note 13). In (A–E), mass differences (in Da) from the expected peak are indicated, and these differences may result from salt adducts or modifications, such as oxidation. Some of the adducted and/or modified peaks appear to have peak overlap as indicated by the peak asymmetry.

13. Process the recorded mass spectra by manually calculating charge state or by using deconvolution software like UniDec (Marty et al., 2015). The UniDec deconvolution parameters used to generate the deconvolved mass spectra in Figs. 2 and 4 are listed in Table 2. The observed masses are reported in Table 3.

Table 2 UniDec parameters used in this method.

Setting	Value	Notes
Data processing		
m/z range	1000–8000	Adjusted to the peak range in each spectrum
Normalize data	On	
Data bin	Nonlinear, 0	
UniDec parameters		
Charge range	1–60	These ranges can be narrowed to be targeted for a known species mass range in a low-complexity spectrum
Mass range	5000–300,000	
Sample mass every (Da)	1	Decrease based on resolution and desired mass accuracy
Peak FWHM (Th)	0.85	
Peak shape function	Gaussian	
Beta	0	Adjusted to 50 for spectra with broad peaks
Charge smooth width	1	
Point smooth width	1	Adjusted to 100 for spectra with broad peaks
Mass smooth width	0	
Maximum # of iterations	100	
m/z to mass transform	Smart	
Adduct mass (Da)	1.007276467	The charge carrier (proton) in positive mode ESI
Manual mode	Off	Manual mode turned on to assign the +29 and +36 peaks in the POP5·RPP30 sample
Native charge offset range	±1000	
Peak selection and plotting		Adjusted to label peaks in the mass spectra

Table 3 Expected and observed masses of *M. maripaludis* RNase P subunits.

Subunit	Determined (Da)	Expected (Da)	Difference (Da)
RPP21 + Zn	12,953 ± 0	12,952	1
RPP29	11,349 ± 0	11,350	−1
L7Ae	12,249 ± 0	12,250	−1
2 L7Ae	24,498 ± 4	24,498	0
2(POP5·RPP30)	83,522 ± 49	83,201	321
4(POP5·RPP30)	168,346 ± 474	166,404	1942
6(POP5·RPP30)	252,289 ± 406	249,606	2683
POP5	15,148 ± 0	15,149	−1
RPP30	26,450 ± 1	26,452	−2
RPR	81,683 ± 3	81,582	101

3.5 Reconstitution of *M. maripaludis* RNase P

An example cleavage assay mix is tabulated below. Step-by-step preparation of assay components, execution of the assay, and analysis of the data are detailed in the text that follows.

Component	Initial concentration	Volume (μL)	Final concentration
Reaction buffer	–	5	–
Folded RPR	6.25 nM	2	0.625 nM
POP5·RPP30	312.5 nM	2	31.25 nM
RPP21	312.5 nM	2	31.25 nM
RPP29	312.5 nM	2	31.25 nM
L7Ae	312.5 nM	2	31.25 nM
Pre-tRNA mix	2 μM; 1600 dpm/μL	5	500 nM; 400 dpm/μL[a]

[a]Quenching 2.5–5 μL will allow loading of 1000–2000 disintegrations per minute (dpm) per well (see Note 23).

1. To fold the RPR, transfer a small aliquot of RPR to a thin-walled 0.5-mL PCR tube.
2. Transfer the PCR tube to a thermocycler, and incubate at 50 °C for 50 min.

3. Drop the temperature to 37 °C, and incubate for 10 min.
4. Add one volume of 2× assay buffer to the RPR, and continue incubating at 37 °C for an additional 30 min.
5. Remove the PCR tube from the thermocycler, and keep the folded RPR at RT.
6. Dilute the folded RPR to 6.25 nM using 1× assay buffer.
7. Remove purified RPP stocks from −20 °C, and keep on ice.
8. Dilute small aliquots of each of the RPP stocks to 312.5 nM using RPP dilution buffer. Add BSA to a final concentration of 0.1 mg/mL to each of the RPP dilutions. Keep the dilutions on ice.
9. Prepare reaction buffer consisting of 1× assay buffer, glycerol, and BSA. The amount of glycerol and BSA added to the reaction buffer should be adjusted so that the final glycerol and BSA concentrations are 2.5% (v/v) and 0.1 mg/mL, respectively, in the final assay mix.
10. In a thin-walled 0.5 mL PCR tube, prepare pre-tRNA mix consisting of 1× assay buffer, unlabeled pre-tRNA substrate, and trace amounts of 5′-[γ-^{32}P]-radiolabeled or internally-[α-^{32}P]-radiolabeled pre-tRNA substrate (see Notes 10 and 23).
11. Mix the folded RPR (final concentration 0.625 nM), RPPs (final concentration 31.25 nM each), and reaction buffer in a thin-walled 0.5 mL PCR tube, and incubate in a thermocycler at 37 °C for 5 min.
12. During the last minute of the incubation in step 11, transfer the PCR tube containing the pre-tRNA mix to the thermocycler, and incubate at 37 °C for 1 min.
13. At the end of the 5 min incubation in step 11, transfer an aliquot of the pre-tRNA mix to the tube containing the RPR and RPPs, and mix by pipetting to initiate the pre-tRNA cleavage reaction.
14. At predetermined time points (see Note 24), remove an aliquot of the assay mix, and transfer it to tubes containing quench dye.
15. Load the quenched reaction samples onto an 8% (w/v) polyacrylamide (19:1 acrylamide:bisacrylamide), 7 M urea gel (16.5 cm × 16.5 cm), and electrophorese using 1× TBE as running buffer.
16. Once the bromophenol blue dye reaches 0.5–1 in. from the bottom of the 16.5 cm × 16.5 cm gel, terminate electrophoresis.
17. Carefully wrap the gel in plastic wrap.
18. Transfer the wrapped gel to a storage phopshor cassette, and expose it to a storage phosphor screen for the desired amount of time (see Note 25).
19. Scan the storage phosphor screen using a phosphorimager instrument, such as a Typhoon RGB (Cytiva) to obtain an image displaying the

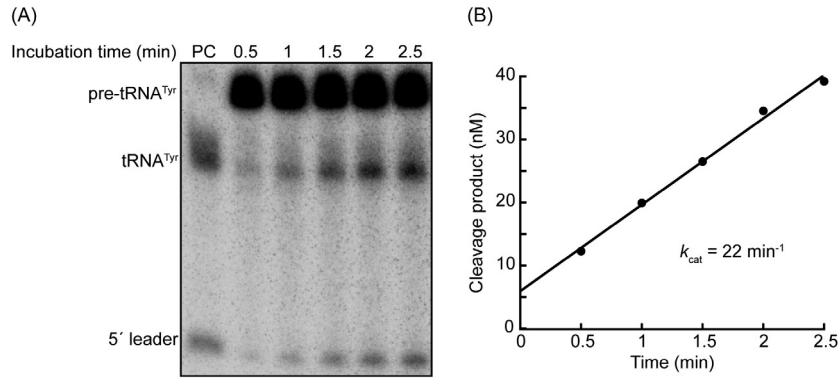

Fig. 3 Measuring the pre-tRNA cleavage activity of *M. maripaludis* RNase P. (A) Representative 8% (w/v) polyacrylamide, 7 M urea gel image illustrating cleavage of 250 nM *E. coli* pre-tRNA^{Tyr} by 0.625 nM *M. maripaludis* RNase P (RPR + 5 RPPs). A trace amount of internally-[α-^{32}P]-radiolabeled pre-tRNA^{Tyr} was added to the assay mix to track the progress of the cleavage reaction. The PC (positive control) lane contains substrate that was cleaved for 15 min at 37 °C by *E. coli* RNase P. The cleavage products in this lane serve as migration markers to confirm that *M. maripaludis* RNase P cleaves the pre-tRNA substrate at the expected site. (B) Representative plot of cleavage product concentration vs time. The volumes of each of the bands in (A) were calculated using ImageQuant software (Molecular Dynamics). The percentage of cleavage product at each time point was calculated using the band volumes as follows: %cleavage = [(tRNA^{tyr}) + (5′ leader)]/[(pre-tRNA^{Tyr}) + (tRNA^{Tyr}) + (5′ leader)]. The resulting values were multiplied by the total substrate concentration at the beginning of the reaction (250 nM). The resulting concentrations are plotted against time. A straight line was fit to the data, and the resulting slope was divided by enzyme concentration to yield k_{cat}.

migration of the radiolabeled pre-tRNA substrate and RNase P-mediated cleavage products (Fig. 3A).

20. Using software such as ImageQuant (Molecular Dynamics), determine the volumes of the substrate and product bands. The measured volumes can be used to calculate the concentration of cleaved pre-tRNA substrate as a function of time.
21. Using data analysis software such as Kaleidagraph (Synergy Software), plot cleavage product concentration vs time, and fit a straight line to the data to obtain initial velocity (Fig. 3B).

3.6 Assessing RPP oligomerization by mass photometry

1. Clean glass slides by sonicating them in 50% (v/v) methanol twice for 30 min each using a water bath sonicator.
2. Sonicate the glass slides in 100% (v/v) methanol twice for 30 min each.

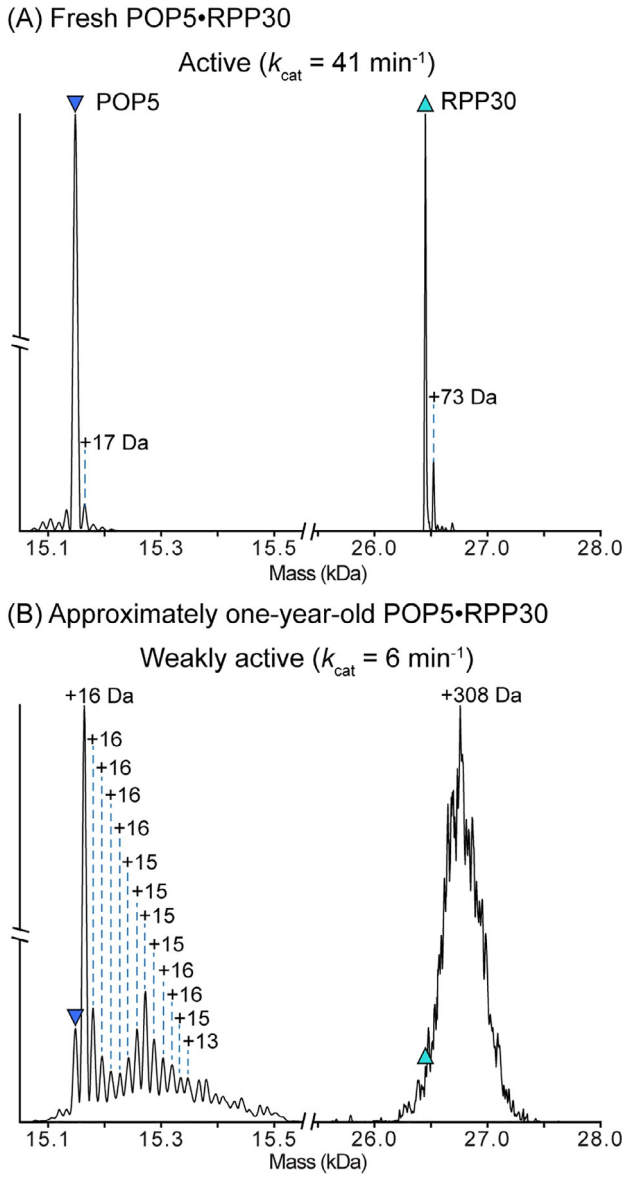

Fig. 4 Deconvolved zero-charge mass spectra after quadrupole isolation and HCD dissociation of a $(POP5{\cdot}RPP30)_2$ charge state. The same preparation of POP5·RPP30 was analyzed and dissociated within (A) 1 month and (B) approximately 1 year after overexpression and purification. Purified POP5·RPP30 is stored at −20 °C as described in

(Continued)

3. Rinse the glass slides with ddH_2O, and then dry with nitrogen gas.
4. Prepare sample wells by slicing CultureWell™ reusable gaskets into groups of four wells each.
5. Clean the gaskets by submerging them in 100% (v/v) isopropyl alcohol for 3 min and then rinsing with ddH_2O. Repeat this washing step four times. Store the gaskets in ddH_2O until ready to use.
6. Dry a single gasket with compressed air.
7. Place the gasket onto the glass slide with the wells facing up.
8. Place a single drop of immersion oil on the sample stage.
9. Place the gasket-containing slide on top of the oil drop. Move the slide to position a well over the center of the sample stage.
10. Aliquot 20 μL of sample (see Note 26) into the well and focus the optics on the droplet.
11. Collect mass photometry data in the ratiometric mode for 1–2 min using the Refeyn AcquireMP software.
12. Analyze, calibrate, and plot the data in the Refeyn DiscoverMP software.
13. Fit the plotted mass distribution to a Gaussian curve (or multiple Gaussian curves for a multimodal mass distribution) to calculate the average measured mass and the standard deviation (Fig. 5).

Fig. 4—Cont'd Section 3.3.1. Prior to analysis, POP5·RPP30 was dialyzed into 500 mM ammonium acetate. After 1 month (A), nearly all of the POP5 and RPP30 have the expected mass, indicating the majority of the protein in solution is unmodified. However, after 1 year (B), both proteins in the complex are heavily modified. The major POP5 peak now shows a single oxidation (+16 Da), and the presence of multiple additional masses correspond to further oxidations. Observed peak overlap and the peak distribution suggest that POP5 likely has other adducts and/or modifications that cannot be assigned. Similarly, the molecular weight of RPP30 has shifted by an average of +308 Da. The unresolved peaks suggest heterogeneous mass additions, which may include modifications, such as oxidation, and other tightly-bound adducts. *M. maripaludis* POP5 contains five Cys, Met, and Trp residues, which are among the most readily oxidizable amino acids (Raftery, 2014). RPP30 has eight such residues. Thus, oxidation is a likely route for modification of these two protein subunits (RPP21 and RPP29 are similarly modified; data not shown). As indicated by the k_{cat} values above each spectrum, the activity of *M. maripaludis* significantly decreases over time, perhaps due to modification of the protein subunits during storage.

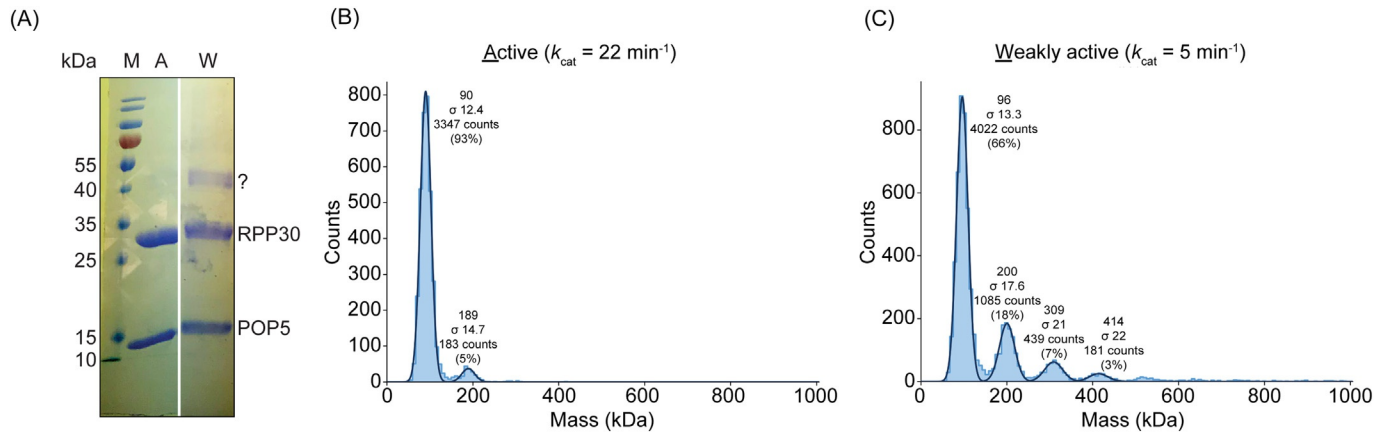

Fig. 5 Oligomerization of *M. maripaludis* POP5·RPP30 analyzed by SDS-PAGE and mass photometry. (A) SDS-PAGE (15% [w/v] polyacrylamide) analysis to compare active (A) and weakly active (W) preparations of POP5·RPP30. The gel image was spliced to position lanes of interest adjacent to each other, but no other adjustments were made. Although there is essentially no difference between the two preparations in the mobilities and relative intensities of the POP5 and RPP30 bands, the weakly active preparation has bands that migrate between the 40 and 55 kDa markers (M), likely corresponding to a heterodimer given the expected molecular weight of POP5·RPP30. The same two preparations of POP5·RPP30 (150 nM each) were diluted in 1× assay buffer (see Section 2.5) and analyzed by mass photometry (B and C). Histogram plotting and fitting was performed in DiscoverMP. The average mass of each population (in kDa), determined by the Gaussian fits, are indicated above each peak. For mass calculation, the following calibrants were used: lens epithelium-derived growth factor, LEDGF (60.4 kDa); bovine serum albumin, BSA (68.5 kDa); HIV integrase (80.4 kDa, monomer; 160.8 kDa, dimer); dihydroorotate dehydrogenase B (237 kDa); apoferritin (480 kDa); thyroglobulin (670 kDa). (B) Mass photometry analysis of an active preparation of POP5·RPP30. The major species (93%) corresponds to the POP5·RPP30 heterotetramer, which is the expected oligomeric state. A minor population of octamer (5%) is also observed. (C) Mass photometry analysis of a weakly active preparation of POP5·RPP30. While the major species is the heterotetramer (66%), the remaining species (29%) are octamer or larger.

4. Notes

1. Fresh DTT is required for the full activity of T7 RNAP. DTT solution stocks should be frozen at −20 °C for long-term storage.
2. When preparing fresh NTP stock solutions from solid, it is important to adjust the pH to ~7 using NaOH. If the pH is not adjusted, the final pH of the IVT reaction will be acidic (due to the high final concentration of NTPs), thus impairing the activity of T7 RNAP and leading to an overall low RNA yield.
3. While a standard NTP mix contains each nucleotide at a concentration of 25 mM, the RNA yield can often be improved by adjusting the concentrations of individual NTPs to match the GC content of the target RNA transcript.
4. IVT templates can be cloned into a plasmid under the control of the T7 promoter sequence and upstream from a (preferably type IIS) restriction enzyme recognition sequence (Vioque, Arnez, & Altman, 1988). Accordingly, restriction digestion of the plasmid will generate a linear DNA template for run-off transcription in which T7 RNAP-mediated transcription is terminated when the polymerase reaches the end of the linear template. Alternatively, an IVT template can be prepared by performing a PCR reaction in which the template sequence (encoded in a plasmid or in a linear double-stranded DNA) is amplified using a forward primer that contains the T7 promoter sequence followed by the 5′ end of the gene, and a reverse primer that is complementary to the 3′ end of the gene.
5. Recombinant T7 RNAP can be purchased or overexpressed and purified in-house. In the latter case, the optimal amount of T7 RNAP to add to a transcription reaction to maximize RNA yield must be empirically determined by performing test IVT reactions containing varying amounts of T7 RNAP (Lyon & Gopalan, 2018).
6. While POP5·RPP30 from all archaea tested thus far readily copurify when cooverexpressed (Chen et al., 2010), RPP21 and RPP29 copurify in only a few systems. In the case of *M. maripaludis*, the two proteins become separated during column chromatography, and therefore cannot be copurified (Cho et al., 2010). Regardless, both proteins are soluble on their own.
7. At pH ~8 and high ionic strength (e.g., >1 M NaCl), PEI will precipitate contaminating RNAs, which can then be removed by

centrifugation. Importantly, minimizing nucleic acid contaminants is critical for active RNase P assembly.

8. Similar columns that are compatible with the FPLC system of choice may be substituted.
9. *E. coli* pre-tRNA^{Tyr} is effectively cleaved by *M. maripaludis* RNase P and other *in vitro* reconstituted archaeal RNase P holoenzymes (Chen et al., 2010; Tsai et al., 2006).
10. Pre-tRNA substrates can be radiolabeled using one of two strategies. First, substrates can be radiolabeled internally by supplementing a trace amount of a single α-^{32}P-radiolabeled NTP into the IVT reaction used to synthesize pre-tRNA. Second, substrates can be 5′-radiolabeled by first dephosphorylating the IVT-synthesized pre-tRNA with calf intestinal alkaline phosphatase. The dephosphorylated pre-tRNA can then be re-phosphorylated by T4 polynucleotide kinase in the presence of trace amounts of γ-^{32}P-radiolabeled ATP. Regardless of the radiolabeling strategy, the radiolabeled pre-tRNAs should be gel-purified to remove excess radiolabeled NTPs and any abortive transcription products.
11. As an alternative to radiolabeling, pre-tRNAs can be detected by using a fluorescent dye to directly label [e.g., fluorescein (Howard et al., 2016)] or stain [e.g., SYBR Gold (ThermoFisher)] the pre-tRNA.
12. The optimal amount of IVT template to maximize RNA yield must be empirically determined by performing test IVT reactions containing varying amounts of template. In general, we have been successful using 4–5 μg of 3000 bp DNA template in a 100 μL IVT reaction.
13. The full-length *M. maripaludis* RPR migrates slower than a 200 bp double-stranded DNA marker on a 2% (w/v) agarose gel. Occasionally, the RPR may migrate as a doublet, which indicates conformational heterogeneity. If such a migration pattern is observed, heat a small aliquot of the RPR for 30 min at 65 °C and then 10 min at 37 °C before gel electrophoresis. In cases where such a treatment does not collapse the doublet into a single band on an agarose gel, denaturing PAGE or native MS can be used to confirm that a single major RNA species is present (Fig. 2F).
14. Although two EtOH washes suffice for many uses, we strongly recommend a third wash for applications that are particularly sensitive to salts (including native MS).
15. Omission of 1% (w/v) glucose from the seed culture results in reproducibly longer growth times to reach the appropriate OD_{600} for induction (~5–6 h vs 2–3 h).

16. After resuspending the pellet, some material may not dissolve. This insoluble matter can be removed by an additional round of centrifugation.
17. *M. maripaludis* RPP stocks (>50 μM) were reported to retain full activity for several months when stored at −20 °C (Cho et al., 2010).
18. RPP29 and L7Ae have very low extinction coefficients, rendering difficult measurement of their concentrations, especially for dilute protein stocks. Use centrifugal concentrators to concentrate stocks in order to obtain reliable absorbance measurements.
19. Thrombin cleavage activity is optimal in 1× PBS, so RPP29 is first dialyzed into 1× PBS before thrombin is added to catalyze removal of the N-terminal $(His)_6$ tag.
20. It is critical that all nonvolatile buffer components are removed and replaced with a volatile salt (e.g., ammonium acetate). The presence of nonvolatile salts will cause ion suppression and adduct formation thereby complicating native MS spectra and data analysis.
21. To ensure the solution is completely at the tip (sharp end) of the emitter, tape the emitter (tip down) to a mini centrifuge rotor and spin briefly at a low RPM.
22. HCD or other types of collisional activation (collision-induced dissociation, CID; in-source trapping; surface-induced dissociation, SID) can be used to dissociate a complex. Alternatively, collisional activation at lower voltages that do not cause complex dissociation or covalent fragmentation can be used to de-adduct and sharpen peaks. This de-adducting, sometimes referred to as "collisional cleaning", is especially useful for accurate mass measurements, particularly in the case of RNAs which retain salts introduced during synthesis and purification steps. The collision voltages needed for dissociation and collisional cleaning are highly sample-dependent; scanning across a range of voltages is recommended.
23. For sensitive gel-based analysis of pre-tRNA substrate and cleavage products, the amount of radiolabeled pre-tRNA substrate added to the reaction should be adjusted so that quenched reaction aliquots loaded onto the urea–PAGE gel contain at least 1000–2000 dpm per lane.
24. To obtain an accurate measurement of the reaction velocity, it is ideal to measure reaction progress when less than 25% of the substrate has been converted to product.
25. To obtain the highest quality gel image, exposure time should be adjusted based on the dpm of the radiolabeled tRNA substrate loaded

onto the gel. However, if the dpm loaded is low (<1000 dpm), longer exposures will also significantly increase background.

26. Sample concentration for mass photometry analysis depends on the sample identity. Data quality will be low at high sample concentrations (>1 μM). We recommend starting at 500 nM and then gradually diluting the sample to optimize data quality.

5. Conclusions

We have presented protocols for purification, reconstitution, and mass analysis of all six subunits (one RNA, five proteins) of RNase P from an archaeon. We emphasize a tag-less approach to protein purification to minimize the potential interference by tags or their remnants during reconstitution of any RNP from constituent subunits prepared by affinity chromatography. We demonstrate the use of MS and MP as complementary approaches for obtaining mass information on the subunits of archaeal RNase P, including accurate molecular weight, metal ion-binding, and oligomeric state. These analyses provided some unexpected insights to better understand the time-dependent decrease in the activity of reconstituted *M. maripaludis* RNase P.

Comparison of fresh or aged protein preparations by MS revealed that the proteins are modified significantly even when stored long-term at −20 °C. For example, in a single preparation of POP5·RPP30, both subunits had several modifications after a year of storage (Fig. 4); in the case of POP5, oxidation seems likely given the step-wise addition of 16 Da to the expected mass. Second, we examined two preparations of POP5·RPP30 that exhibited a sevenfold difference in activities in the reconstituted holoenzymes. MP clearly reveals that, under conditions comparable to those used in activity assays, there are differences in the distributions of the oligomeric states present in these two preparations (Fig. 5). While the linkage (if any) between oxidation and oligomerization (or vice versa) remains to be determined, these two methods provide insights into sample heterogeneity that is not easily obtained by other means. For example, biochemists rely heavily on SDS-PAGE, a convenient method for establishing molecular weights and protein degradation, but oxidations and nonnative oligomerizations are likely to go undetected with this method. With insights from MS and MP, customized preventive measures could be implemented to extend protein shelf life (e.g., flushing stock tubes of protein with argon or adding a small amount of nonionic detergent).

The growing appreciation of the roles of long noncoding (lnc) RNAs and lncRNA–protein complexes in diverse cellular processes heightens the need for information and insights that will facilitate biochemical and biophysical studies of RNPs. Our findings on *M. maripaludis* RNase P are likely to be instructive in this regard.

Acknowledgments

We are grateful for research funding from the National Institutes of Health [GM120582 to V.G. and V.H.W.; P41GM128577 to V.H.W.] and from the OSU Comprehensive Cancer Center for a Pelotonia Post-doctoral Fellowship [W.J.Z.]. We thank Richard Fishel and Ross Larue for training and use of the Refeyn One mass photometry instrument, funded by NIH grant CA067007 and the James Comprehensive Cancer Center.

References

Altman, S. (2007). A view of RNase P. *Molecular BioSystems*, *3*(9), 604–607. https://doi.org/10.1039/b707850c.

Chen, W. Y., Pulukkunat, D. K., Cho, I. M., Tsai, H. Y., & Gopalan, V. (2010). Dissecting functional cooperation among protein subunits in archaeal RNase P, a catalytic ribonucleoprotein complex. *Nucleic Acids Research*, *38*(22), 8316–8327. https://doi.org/10.1093/nar/gkq668.

Chen, W. Y., Singh, D., Lai, L. B., Stiffler, M. A., Lai, H. D., Foster, M. P., et al. (2012). Fidelity of tRNA 5′-maturation: A possible basis for the functional dependence of archaeal and eukaryal RNase P on multiple protein cofactors. *Nucleic Acids Research*, *40*(10), 4666–4680. https://doi.org/10.1093/nar/gks013.

Cho, I. M., Lai, L. B., Susanti, D., Mukhopadhyay, B., & Gopalan, V. (2010). Ribosomal protein L7Ae is a subunit of archaeal RNase P. *Proceedings of the National Academy of Sciences of the United States of America*, *107*(33), 14573–14578. https://doi.org/10.1073/pnas.1005556107.

Esakova, O., & Krasilnikov, A. S. (2010). Of proteins and RNA: The RNase P/MRP family. *RNA*, *16*(9), 1725–1747. https://doi.org/10.1261/rna.2214510.

Evans, D., Marquez, S. M., & Pace, N. R. (2006). RNase P: Interface of the RNA and protein worlds. *Trends in Biochemical Sciences*, *31*(6), 333–341. https://doi.org/10.1016/j.tibs.2006.04.007.

Fukuhara, H., Kifusa, M., Watanabe, M., Terada, A., Honda, T., Numata, T., et al. (2006). A fifth protein subunit Ph1496p elevates the optimum temperature for the ribonuclease P activity from *Pyrococcus horikoshii* OT3. *Biochemical and Biophysical Research Communications*, *343*(3), 956–964. https://doi.org/10.1016/j.bbrc.2006.02.192.

Gopalan, V., Jarrous, N., & Krasilnikov, A. S. (2018). Chance and necessity in the evolution of RNase P. *RNA*, *24*(1), 1–5. https://doi.org/10.1261/rna.063107.117.

Guerrier-Takada, C., Gardiner, K., Marsh, T., Pace, N., & Altman, S. (1983). The RNA moiety of ribonuclease P is the catalytic subunit of the enzyme. *Cell*, *35*(3 Pt. 2), 849–857. https://doi.org/10.1016/0092-8674(83)90117-4.

Howard, M. J., Karasik, A., Klemm, B. P., Mei, C., Shanmuganathan, A., Fierke, C. A., et al. (2016). Differential substrate recognition by isozymes of plant protein-only ribonuclease P. *RNA*, *22*(5), 782–792. https://doi.org/10.1261/rna.055541.115.

Kikovska, E., Svard, S. G., & Kirsebom, L. A. (2007). Eukaryotic RNase P RNA mediates cleavage in the absence of protein. *Proceedings of the National Academy of Sciences of the United States of America*, *104*(7), 2062–2067. https://doi.org/10.1073/pnas.0607326104.

Kouzuma, Y., Mizoguchi, M., Takagi, H., Fukuhara, H., Tsukamoto, M., Numata, T., et al. (2003). Reconstitution of archaeal ribonuclease P from RNA and four protein components. *Biochemical and Biophysical Research Communications*, *306*(3), 666–673. https://doi.org/10.1016/s0006-291x(03)01034-9.

Lai, L. B., Tanimoto, A., Lai, S. M., Chen, W. Y., Marathe, I. A., Westhof, E., et al. (2017). A novel double kink-turn module in euryarchaeal RNase P RNAs. *Nucleic Acids Research*, *45*(12), 7432–7440. https://doi.org/10.1093/nar/gkx388.

Lai, L. B., Vioque, A., Kirsebom, L. A., & Gopalan, V. (2010). Unexpected diversity of RNase P, an ancient tRNA processing enzyme: Challenges and prospects. *FEBS Letters*, *584*(2), 287–296. https://doi.org/10.1016/j.febslet.2009.11.048.

Lai, S.M., Thirugnanasambantham P., Sidharthan V., Norris A.S., Law J.D., Gopalan V., et al. (2021). Use of tandem affinity–buffer exchange chromatography online with native mass spectrometry for optimizing overexpression and purification of recombinant proteins. *Methods in Enzymology*, *659*, 37–70.

Lyon, S., & Gopalan, V. (2018). A T7 RNA polymerase mutant enhances the yield of 5'-thienoguanosine-initiated RNAs. *Chembiochem*, *19*(2), 142–146. https://doi.org/10.1002/cbic.201700538.

Marty, M. T., Baldwin, A. J., Marklund, E. G., Hochberg, G. K., Benesch, J. L., & Robinson, C. V. (2015). Bayesian deconvolution of mass and ion mobility spectra: From binary interactions to polydisperse ensembles. *Analytical Chemistry*, *87*(8), 4370–4376. https://doi.org/10.1021/acs.analchem.5b00140.

Pannucci, J. A., Haas, E. S., Hall, T. A., Harris, J. K., & Brown, J. W. (1999). RNase P RNAs from some Archaea are catalytically active. *Proceedings of the National Academy of Sciences of the United States of America*, *96*(14), 7803–7808. https://doi.org/10.1073/pnas.96.14.7803.

Perederina, A., Berezin, I., & Krasilnikov, A. S. (2018). *In vitro* reconstitution and analysis of eukaryotic RNase P RNPs. *Nucleic Acids Research*, *46*(13), 6857–6868. https://doi.org/10.1093/nar/gky333.

Pulukkunat, D. K., & Gopalan, V. (2008). Studies on *Methanocaldococcus jannaschii* RNase P reveal insights into the roles of RNA and protein cofactors in RNase P catalysis. *Nucleic Acids Research*, *36*(12), 4172–4180. https://doi.org/10.1093/nar/gkn360.

Raftery, M. J. (2014). Determination of oxidative protein modifications using mass spectrometry. *Redox Report*, *19*(4), 140–147. https://doi.org/10.1179/1351000214Y.0000000089.

Soltermann, F., Foley, E. D. B., Pagnoni, V., Galpin, M., Benesch, J. L. P., Kukura, P., et al. (2020). Quantifying protein-protein interactions by molecular counting with mass photometry. *Angewandte Chemie (International Ed. in English)*, *59*(27), 10774–10779. https://doi.org/10.1002/anie.202001578.

Sonn-Segev, A., Belacic, K., Bodrug, T., Young, G., VanderLinden, R. T., Schulman, B. A., et al. (2020). Quantifying the heterogeneity of macromolecular machines by mass photometry. *Nature Communications*, *11*(1), 1772. https://doi.org/10.1038/s41467-020-15642-w.

Studier, F. W., & Moffatt, B. A. (1986). Use of bacteriophage T7 RNA polymerase to direct selective high-level expression of cloned genes. *Journal of Molecular Biology*, *189*(1), 113–130. https://doi.org/10.1016/0022-2836(86)90385-2.

Sun, L., & Harris, M. E. (2007). Evidence that binding of C5 protein to P RNA enhances ribozyme catalysis by influencing active site metal ion affinity. *RNA*, *13*(9), 1505–1515. https://doi.org/10.1261/rna.571007.

Tsai, H. Y., Pulukkunat, D. K., Woznick, W. K., & Gopalan, V. (2006). Functional reconstitution and characterization of *Pyrococcus furiosus* RNase P. *Proceedings of the National Academy of Sciences of the United States of America*, *103*(44), 16147–16152. https://doi.org/10.1073/pnas.0608000103.

Vioque, A., Arnez, J., & Altman, S. (1988). Protein-RNA interactions in the RNase P holoenzyme from *Escherichia coli*. *Journal of Molecular Biology*, *202*(4), 835–848. https://doi.org/10.1016/0022-2836(88)90562-1.

Wan, F., Wang, Q., Tan, J., Tan, M., Chen, J., Shi, S., et al. (2019). Cryo-electron microscopy structure of an archaeal ribonuclease P holoenzyme. *Nature Communications*, *10*(1), 2617. https://doi.org/10.1038/s41467-019-10496-3.